Published in final edited form as:
Am J Physiol Cell Physiol. 2008 June ; 294(6): C1576–C1585. doi:10.1152/ajpcell.00518.2007.

Shear Stress Influences Spatial Variations in Vascular Mn-SOD Expression

Lisong Ai[*,+], **Mahsa Rouhanizadeh**[*,+], **Joseph C. Wu**[#], **Wakako Takabe**[*], **Hongyu Yu**[*], **Mohammad Alavi**[&], **Yi Chu**[&&], **Jordan Miller**[&&], **Donald D. Heistad**[&&], and **Tzung K. Hsiai**[*]

[*]Department of Biomedical Engineering and Cardiovascular Medicine, University of Southern California, Los Angeles, California

[#]Department of Medicine, Division of Cardiology, Stanford University School of Medicine, Stanford, California

[&]Department of Pathology, University of Southern California, Los Angeles, California

[&&]Department of Internal Medicine, University of Iowa Carver College of Medicine and VA Medical Center, Iowa City, Iowa

Abstract

Fluid shear stress modulates vascular production of endothelial superoxide anion ($O_2^{\cdot}$) and nitric oxide ($^{\cdot}NO$). Whether the characteristics of shear stress influence the spatial variations in mitochondrial manganese superoxide dismutase (Mn-SOD) expression in vasculatures is not well-defined. We constructed a 3-D Computational Fluid Dynamics model simulating spatial variations in shear stress at the arterial bifurcation. In parallel, explants of arterial bifurcations were sectioned from the human left main coronary bifurcation and right coronary arteries for immunohisto-localization of Mn-SOD expression. We demonstrated that Mn-SOD staining was prominent in the athero-protective regions, but was nearly absent in the lateral wall of arterial bifurcation. Pulsatile shear stress (PSS: mean shear stress τ_{ave}= 23 dyn·cm^{-2}) up-regulated Mn-SOD mRNA expression at a higher level than did oscillatory shear stress (OSS: τ_{ave}= 0.02 dyn·cm^{-2} ± 3.0 dyn·cm^{-2}·s^{-1} at 1 Hz) in cultured bovine aortic endothelial cells (PSS by 11.3±0.4-fold versus OSS by 5.0±0.5-fold. $p < 0.05$, n=4). Furthermore, PSS decreased the extent of Low Density Lipoprotein (LDL) nitration, whereas OSS increased by Liquid chromatography and tandem mass spectrometry ($P < 0.05$, n=4). Treatment with Mn-SOD siRNA significantly increased intracellular nitrotyrosine level in presence of LDL (n=4, $p < 0.5$). Our findings indicate that shear stress in the athero-prone versus athero-protective regions regulates spatial variations in mitochondrial Mn-SOD expression. Shear stress modulated LDL protein nitration via Mn-SOD expression.

Keywords

Shear stress; Mn-SOD; superoxide anion; nitric oxide; nitrotyrosine

Introduction

Atherosclerotic lesions preferentially develop in the lateral walls of vessel bifurcations and curvatures 1. Predilection sites for atherosclerosis are modulated by flow patterns to which

T. K. Hsiai, M.D., Ph.D., Department of Biomedical Engineering and Division of Cardiovascular Medicine, University of Southern California, Los Angeles, Ca 90081, thsiai@usc.edu.
[+]Both authors contribute equally.

the endothelium is exposed [2,3]. At the lateral wall of arterial bifurcations, a complex flow profile develops; flow separation and migrating stagnation points create oscillating shear stress (i.e., bidirectional with no net forward flow) [4]. Oscillatory shear stress increases oxidative stress which promotes development of atherosclerotic plaque [5–9]. In contrast, pulsatile flow down-regulates adhesion molecules and reactive oxygen species in the medial wall of bifurcations or relatively straight segments.

Mitochondria are important sources of cellular superoxide anion ($O_2^{\cdot -}$) and H_2O_2 as a result of electron transport leak at complex I and III of the respiratory chain [10,11]. Mitochondrial superoxide dismutase (manganese SOD or Mn-SOD) is essential for life. Homozygous mice that are deficient for Mn-SOD die within days of birth [12]. While expression of CuZn-SOD is regulated by blood flow [13–16], it remains undefined if expression of Mn-SOD is influenced by specific shear stress patterns in the athero-prone versus athero-protective regions.

Fluid shear stress influences the relative production of $^{\cdot}NO$ and $O_2^{\cdot}$-[17,18]. In the athero-protective regions, pulsatile shear stress (PSS) up-regulates eNOS phosphorylation mainly via the PI3-akt-mediated pathway [19,20], and down-regulates vascular endothelial NADPH oxidases, a major source of $O_2^{\cdot}$-[18]. In the athero-prone regions, oscillatory shear stress (OSS) down-regulates eNOS activation, and up-regulates NADPH oxidase. OSS also attribute to the imbalance between $O_2^{\cdot}$- and $^{\cdot}NO$ formation (ref: Hsiai, FRBM, 2007), favoring a diffusion-limited reaction to yield a potent oxidant, peroxynitrite ($O_2^{\cdot -} + {}^{\cdot}NO \rightarrow ONOO^-$) [21,22]. Peroxynitrite reacts preferentially with tyrosine residues in proteins leading to 3-nitrotyrosine, a finger print of $ONOO^-$ reactivity. In this context, we examined the spatial variations in Mn-SOD expression in medium-sized conductance blood vessels as a mechanism to influence $ONOO^-$ formation.

In the present study, the dynamic 3-D computational fluid dynamics (CFD) model predicts PSS in athero-protective versus OSS in athero-prone regions. Using the explants of human coronary arterial bifurcations, we assessed whether PSS versus OSS in these two regions influenced Mn-SOD immunohisto-localization. We demonstrated that Mn-SOD staining was prominent in the athero-protective region, but it was nearly absent in the athero-prone regions. Pulsatile shear stress up-regulated Mn-SOD mRNA expression at a higher level than did oscillatory shear stress in cultured bovine aortic endothelial cells. PSS further modulated the extent of LDL protein nitration via Mn-SOD expression. Our findings indicate that the characteristics of shear stress influence spatial variations in Mn-SOD expression with an implication for influencing nitrotyrosine formation.

Methods

Three-Dimensional Bifurcation Model

The novel approach in this study is to link specific shear stress patterns in the athero-protective versus athero-prone regions of a 3-D bifurcation model with the corresponding Mn-SOD and nitrotyrosine localization from the explants of human coronary arteries. In addition, the molecular mechanisms by which specific shear stress patterns modulate endothelial Mn-SOD mRNA expression and LDL protein nitration were elucidated by cultured bovine aortic endothelial cells (BAEC) and/or human aortic endothelial cells (HAEC) in a 2-D dynamic flow system.

Generation of 3-D geometries and meshes—The construction of the bifurcation model and the associated flow patterns have been described previously (1. Bharadvaj, B.K., Mabon, R.F., Giddens, D.P., Steady flow ina model of the human carotid bifurcation. Part I: Flow visualization. Journal of Biomechanics 1982. 15:349–362. 2. Gijsen F.J.H., van de Vosse F.N., Janssen, J., The influence of the non-Newtonian properties of blood on the flow

in large arteries: steady flow in a carotid bifurcation model. Journal of Biomechanics 1999 32: 601–608. 3. Kim CS, Kiris C, Kwak D, David T, Numerical Simulation of Local Blood Flow in the Carotid and Cerebral Arteries Under Altered Gravity, Journal of Biomechanical Engineering, 2006. Volume 128, Issue 2, pp. 194–202). Briefly, the commercial CAD software, Pro Engineer Wildfire V.3.0 (Parametric Technology, Needham, MA), was employed to construct the 3-D luminal geometrical model, which was then imported into a specialized pre-processing program for mesh generation (Fluent Inc., Gambit 2.3.16, Lebanon, NH, USA). The mesh consisted of tetrahedral elements and was imported into the main computational fluid dynamic (CFD) solver (Fluent Inc., Fluent 6.2.16, Lebanon, NH, USA) for flow simulation.

Blood flow model and boundary conditions—The 3-D Navier-Stokes equations were applied to solve the blood flow. The governing equations included mass and momentum equations which were used to solve for laminar, incompressible, and non-Newtonian flow. The arterial wall was assumed be rigid and impermeable. Characteristics such as inlet flow waveforms, blood viscosity, and vessel diameters were controlled in order to achieve the physiological conditions as previously reported in human left carotid artery [1–3]. The pulsatile inlet flow rate was implemented by using 12 harmonics written in a user-defined C ++ code.

Two-Dimensional Flow System

Two-dimensional dynamic flow channels were used to implement pulsatile (PSS) and oscillatory shear stress (OSS) obtained from the 3-D bifurcation model mentioned above. The 2-D flow system provides the precise and well-defined flow profiles across the width of the parallel flow chamber at various temporal variations in shear stress ($\partial\tau/\partial t$), frequency, and amplitude [27]. Bovine aortic endothelial cells were exposed to the characteristics of shear stress as obtained from the 3-D bifurcation model: (1) PSS at a time-averaged shear stress (τ_{ave}) of 23 dyn·cm^{-2} with a temporal gradient ($\partial\tau/\partial t$) of 71 dyn.cm.$^{-2}$.sec^{-1}; and (2) OSS at a τ_{ave} of 0.02 ± 3 dyn·cm^{-2} and $\partial\tau/\partial t$ of 0 dyn.cm.$^{-2}$·sec^{-1}. The 2-D model allowed for real-time monitoring of shear stress and quantitative real-time RT-PCR and Western blots from a sufficient number of vascular endothelial cells (EC) [28,29,30].

Endothelial Cell Culture

Confluent bovine aortic endothelial cells (BAEC) between passages 4 and 7 were seeded on Cell-Tak cell adhesive and Collagen Type I (BD bioscience, San Jose, CA) coated glass slides (5 cm^2) at 3×10^6 cells per slide. BAEC were grown to confluent monolayers in high glucose (4.5 g/L) DMEM (Dulbecco's Modified Eagle's Medium) supplemented with 10% heat-inactivated fetal bovine serum (Hyclone), 100 U/ml L-glutamine-penicillin-streptomycin (Sigma) for 48 h in 5% CO_2 at 37°C.

Immunohistochemistry of Human Coronary Arteries

Three human coronary arteries were obtained from explanted hearts of cardiac transplant patients in compliance with the Institutional Review Board. Cross-sections of the left and right coronary arteries with and without atherosclerotic lesions were analyzed. Monoclonal antibodies were used for Mn-SOD (Upstate). Immunostaining was performed with standard techniques in frozen vascular tissue using biotinylated secondary antibodies and peroxidase staining. Diaminobenzidine (DAB) was used as a chromogen and the sections were counterstained with hematoxylin for visualization of intima, media, smooth muscle cells and adventitia.

Counterstaining was performed to distinguish endothelial (EC) and smooth muscle cells (SMC) in the media and/or intima proximal to the point of flow separation. EC and SMC

were stained with monoclonal antibodies specific for von Willebrand Factor (vWF) (1:25 dilution) and β-actin (1:4000 dilution) (Dakocytomation, Carpinteria, CA). Negative controls were performed by omitting the primary antibody. Positive controls included brain and kidney tissues.

Separation of LDL Subspecies by High-Performance Liquid Chromatography

Venous blood was obtained at the Atherosclerosis Research Unit from fasting adult human volunteers under institutional review board approval. Plasma was pooled and immediately separated by centrifugation at 1500*g* for 10 minutes at 4°C. LDL (δ=1.019 to 1.063 g/mL) was isolated from freshly separated plasma by preparative ultracentrifugation using a Beckman L8-55 ultracentrifuge and a SW-41 rotor. The technique used for separating LDL was similar to that described previously [31].

Endothelial Cell Exposure to Shear Stress

A dynamic flow system was used to implement temporal variations in shear stress ($\partial\tau/\partial t$); namely, pulsatile (PSS) and oscillatory (OSS) shear stress 28،29،30. Confluent BAEC were exposed to the flow conditions in the absence and presence of native LDL (50 μg/mL). After 4 hours, BAEC were collected for quantitative real-time RT-PCR and Western blots. In the presence of LDL, the culture medium was collected to measure apo-B-100 nitration of the tyrosine residues.

Quantitative Real-Time RT-PCR

Confluent bovine aortic endothelial cell (BAEC) monolayers were exposed to PSS and OSS in a parallel plate flow system for 4 hours as mentioned above. Total RNA was isolated using the RNeasy kit (Qiagen). RNA was reverse-transcribed, followed by PCR amplification using the SuperScript III Platinum two-Step qRT-PCR Kit with SYBR Green (Invitrogen, Carlsbad, CA). Oligonucleotides for Mn-SOD were (1) forward primer 5´-GGA AGC CAT CAA ACG TGA CT-3´ and (2) reverse primer 3´-AGC AGG GGG ATA AGA CCT GT-5´. Fidelity of the PCR reaction was determined by melting temperature analysis. For quantification of relative gene expression, the target sequence was normalized to 18s rRNA. The difference in C_T values for various flow conditions vs. control was used to determine the relative difference in the levels of Mn-SOD mRNA expression.

LDL Protein Nitration

LDL suspended in medium was collected for analysis of protein nitration. Protein-bound nitrotyrosine formation in the recovered media was determined by stable isotope dilution liquid chromatography–tandem mass spectrometry [32] on a mass spectrometer (API 4000, Applied Biosystems, Foster City, CA) interfaced with a Cohesive Technologies Aria LX Series HPLC multiplexing system (Franklin, MA). Synthetic $^{13}C_6$-labeled nitrotyrosine internal standard was added to samples for quantification of natural abundance of analytes. Simultaneously, a universal labeled precursor amino acid, $^{13}C_9$,$^{15}N_1$ tyrosine (for nitrotyrosine) was added to quantify the precursors and to assess potential intra-preparative artifactual oxidation during sample handling and analysis. Proteins were hydrolyzed under argon atmosphere in methane sulfonic acid, and then samples passed over mini solid-phase C18 extraction columns (Supelclean LC-C18-SPE minicolumn; Supelco, Inc., Bellefone, PA) prior to mass spectrometry analysis. Results were normalized to the content of the precursor amino acid, which was monitored within the same injection. Formation of $^{13}C_9$,^{15}N-labeled nitrotyrosine was routinely monitored and negligible (i.e. < 5% of the level of the natural abundance product observed).

Analysis for Nitrotyrosine

Confluent BAEC at fourth passage were pretreated with diethyldithiocarbamic acid (DIECA), a copper chelator to inhibit CuZn-SOD (1mM for 60 minutes), and/or MnTMPyP, a Mn-SOD mimetic (10 μM for a 30 minutes) in a serum-free DMEM medium. After washing DECT and/or MnTMPyP with PBS, BAEC were incubated with native LDL at 50 μg/mL for 4 hours. LDL suspended in mediums was collected to assess LDL protein nitration. LDL in the medium was concentrated by centrifugation at 3,000 rpm in Centriprep Centrifugal Filter Devices with YM-30 MW (Millipore). Dot blots were performed by spotting 15 μg of LDL. Membranes were soaked in methanol and washed with TBS-T. Samples were blocked in BSA and incubated with a polyclonal nitrotyrosine antibody overnight (1:3000 dilution, Upstate, NY), followed by incubation with horseradish-peroxidase-HPR-conjugated goat ant-rabbit secondary antibody (1:10000). Blots were detected using ECL chemiluminescence kit (Pierce, Rockford, IL). Positive control was established by treating LDL (0.2 mg/mL) with peroxynitrite at 100 μM.

Silencing Mn-SOD mRNA in Human Aortic Endothelial Cells

Silencer siRNA was custom-designed for Mn-SOD by Ambion (Austin, TX). The sense sequence was: GGCCUGAUUAUCUAAAAGCtt and that of the anti-sense was: GCUUUUAGAUAAUCAGGCCtg. Confluent human aortic endothelial cells (HAEC) monolayers from passages 4 to 9 were trypsinized and re-suspended in standard growth medium to 100,000 cells/mL. siPORT NeoFX transfection reagent was diluted in OPTIMEM medium and incubated at room temperature for 10 minutes. Mn-SOD siRNA at a final concentration of 30 nM was diluted in OPTIMEM and mixed with diluted siPORT NeoFX reagent at room temperature for additional 10 minutes. The transfection solution was dispensed into the 6-well plates, followed by adding HAEC in suspension. The medium was changed to standard growth medium after 24 hours. The medium was replaced every other day until confluent HAEC monolayers developed. Quantitative RT-PCR and dot blot were performed to validate effective silencing of Mn-SOD.

Western Analysis for Intracellular Nitrotyrosine Level

HAEC and siMn-SOD-treated HAEC were incubated with the CuZn-SOD chelator, diethyldithiocarbamic acid (DIECA) at 10μM. The third HAEC sample was treated with the Mn-SOD mimetic, MnTMPyP, 10 μM. After 1 hour, the control sample (HAEC only) and the treated samples were incubated with LDL at 50μg/ml. A blank sample was not treated with LDL or any other treatment. A positive control was treated with LDL, followed by $ONOO^-$ (100 μM). After 4 hours, the cell lysates were collected. The Western analyses for nitrotyrosine were performed at a 1:3000 dilution in TBS-Tween for primary monoclonal nitrotyrosine antibody (Upstate Cell Signaling Solutions) and 1:10000 dilution for anti-mouse secondary antibody as previously described [33]. Densitometry was performed using an NIH Scion Image Software (Scion Corp., Frederick, MD).

Statistical Analysis

Data are expressed as mean ± SD and compared among separate experiments. For comparisons between two groups, two-sample independent-groups t-test was used. Comparisons of multiple values were made by one-way analysis of variance (ANOVA), and statistical significance among multiple groups determined using the Tukey test (for pairwise comparisons of means between static-like and pulsatile flow conditions). *P*-values of < 0.05 are considered statistically significant.

Results

Characteristics of Mean Shear Stress in a 3-D Bifurcation Model

The intention of our 3-D model was developed to link between specific shear stress profiles and spatial variations in Mn-SOD expression with an implication for spatial variation for nitrotyrosine formation. The dynamic 3-D CFD code demonstrated shear stress at the lateral versus medial wall of internal and external carotid arteries, and the divider of the bifurcation using non-Newtonian blood flow (Bird R. B., Armstrong R. C., Hassager O., 1977. Dynamics of Polymeric Liquids, Vol. 1, Fluid Mechanics New York: Wiley. 470 PP.) (Figs. 1a–c). At a given instantaneous moment (t = 0.244 seconds), magnitude of shear stress was the highest at the divider of bifurcation and lowest at the point of flow separation. For a Reynolds number of 289, the time-averaged shear stress of pulsatile flow along the medial wall of internal carotid artery ranged from 20 to 26 dynes·cm^{-2} (Figs. 1e and 1f). The point of flow separation oscillated between −3 and 3 dynes·cm^{-2} in response to cardiac contraction. The shear stress valves derived from the 3-D CFD code provided a basis to assess spatial variations in Mn-SOD expression.

Spatial Variations in Mn-SOD and nitrotyrosine Immunostaining

In the present study, Mn-SOD staining was absent in the OSS-exposed regions, but it was prominent throughout the entire endothelium in the PSS-exposed regions without disease (Fig. 2). Von Willebrand staining (vWF) and eNOS staining was positive in the entire luminal EC in the PSS-exposed region [33]. In contrast, nitrotyrosine staining was prominent in the arterial bifurcation regions where eNOS and Mn-SOD staining were nearly absent (Fig. 3). The integration of CFD and immunohisto-localizations suggests that spatial variation in Mn-SOD expression is regulated by the specific shear stress patterns. We have recently reported that nitrotyrosine immunohisto-staining was prominent in the OSS-exposed regions, but absent in the PSS-exposed regions (*Hsiai, FRBM, 2007*). Our present study supported the notion that Mn-SOD staining was prominent in the PSS-exposed regions where nitrotyrosine was nearly absent, but Mn-SOD was absent in the OSS-exposed regions where nitrotrosine was prominent.

Flow Regulation of Mn-SOD mRNA Expression and Nitrotyrosine Formation

BAEC were exposed to shear stress in a dynamic flow system simulating flow profiles in the PSS- and OSS-exposed regions of 3-D arterial bifurcation. Endothelial Mn-SOD mRNA was significantly up-regulated in response to shear stress. Specifically, PSS induced an 11.3-fold increase while OSS induced a 5-fold increase (Fig. 4b). Western blots supported the trend in Mn-SOD mRNA expression (Fig. 4d). CuZn-SOD mRNA expression was also increased by 2.3-fold in response to PSS (Fig. 4a). However, EC-SOD remained unresponsive to shear stress (Fig. 4c). To test the pathophysiologic significance of Mn-SOD expression, we assessed LDL particles as a surrogate marker for protein nitration by $ONOO^-$ (*Hsiai, FRBM, 2007*). The LDL apoB-100 residues were analyzed by liquid chromatography / electro spray ionization / tandem mass spectrometry (LC/ESI/MS/MS). OSS increased the level of protein nitration while PSS significantly decreased the level in comparison with the control under static conditions (Fig. 5).

The Effects of Mn-SOD siRNA on Extra- and Intra-Cellular Nitrotyrosine Levels

To further test the antioxidant nature of Mn-SOD, we silenced Mn-SOD (Mn-SOD siRNA) in HAEC. SiMnSOD-treated HAEC were then incubated with native LDL. Dot blot analysis for extracellular ONOO- demonstrated that MnTMPyP, a Mn-SOD mimetic, reduced LDL nitration (Fig. 6). Nitrotyrosine level in siMn-SOD treated HAEC was significantly higher than that of MnTMPyP-treated HAEC. Intracellular nitrotyrosine levels were also assessed

in siMn-SOD-treated HAEC (Fig. 7). Mn-SOD siRNA significantly increased intracellular nitrotyrosine level in comparison with native LDL-treated BAEC. Our observation corroborated the notion that Mn-SOD expression influenced the extent of LDL protein nitration, and that pulsatile shear stress attenuated the extent of LDL nitration via Mn-SOD up-regulation. Thus, our CFD code enabled us to link specific shear stress profiles with spatial variations in Mn-SOD expression with an implication for nitrotyrosine formation.

Discussion

In this study, we demonstrated that shear stress influenced spatial variations in Mn-SOD expression. That oscillatory and pulsatile shear stress patterns may contribute to this phenomenon is supported by three lines of evidences: (1) the 3-D computational fluid dynamic model predicts regions of OSS and PSS in the arterial bifurcations; (2) immunohisto-localization and physiological study showed that Mn-SOD staining was prominent in the PSS-exposed regions where nitrotyrosine staining was absent, (3) using a 2-D flow system, we demonstrated that PSS and OSS differentially regulated LDL protein nitration via Mn-SOD mRNA expression.

The 3-D CFD code confirmed that the endothelial cells (EC) in medial wall or the straight segment of vessels experience pulsatile shear stress (PSS); whereas EC near the point of flow separation experience oscillatory shear stress (OSS) in the atherosclerosis-prone regions [1]. The mean shear stress values obtained from the 3-D model were implemented in the 2-D flow system to elucidate SOD isoform mRNA expression and LDL protein nitration. Our dynamic model was designed to generate specific pulsatile versus oscillatory shear stress at various slew rates (*Hsiai, Ann BME, 2002*); however, Blackman *et al*. reported the atheroprotective versus athero-genic waveforms from human carotid arteries (*ref-Blackman BR, 2002*).

Mn-SOD is an important dismutase of reactive oxygen species acting in the mitochondria matrix. Oxidative phosphorylation in mitochondria ATP occurs as electrons are transferred from NADH or $FADH_2$ to molecular oxygen. The transfer of more than 98% of electrons by the electron transport chain is coupled with the production of ATP, 1.5 to 2 % of electrons leak out to form $O_2^{\cdot -}$, which is dismutased by Mn-SOD [34]. In response to pathologic conditions such as reperfusion injury, the electron transport chain may become uncoupled, leading to an increase in $O_2^{\cdot -}$ production [35]. Bernal-Mizrachi *et al*. reported respiratory uncoupling in smooth muscle cells caused atherosclerosis in mice [36]. In apolipoprotein E (apoE)-deficient mice (apoE(−/−))[37], the normally expressed levels of Mn-SOD protects against oxidative stress and endothelial dysfunction.

We were able to compare the OSS-exposed regions such as bifurcations or greater curvatures with the PSS-exposed regions such as the relative straight segments or medial wall of arterial bifurcations. Our finding supports the notion that spatial variations in shear stress influence MnSOD staining in 3 out of 3 explants of human coronary arteries. All three patients were diagnosed with ischemic cardiomyopathy due to atherosclerosis. The immunohistochemistry analysis in figure 2 was representative of a section of left anterior distal arteries where pulsatile shear stress occurred and atherosclerotic lesions were absent; and that of figure 3 was representative of lateral wall of an arterial bifurcation where oscillatory shear stress developed and atherosclerotic lesions were present. We previously reported that nitrotyrosine staining was prominent in the OSS-exposed region, but it was absent in the PSS-exposed regions [33]. In PSS-exposed regions, Mn-SOD staining was prominent but nitrotyrosine staining was absent, and Mn-SOD expression influenced the extent of LDL nitration (Figs. 5 & 6).

Our data also suggest that Mn-SOD and CuZn-SOD, but not EC-SOD, are responsive to shear stress in vascular endothelial cells. EC-SOD is synthesized in smooth muscle cells, and CuZn-SOD is prevalent in vascular endothelial cells. Inou *et al.* reported that CuZn-SOD in human aortic endothelial cells (HAEC) is up-regulated in response to laminar flow [13]. Despite different experimental designs; namely, (1) the cell type (BAEC versus HAEC), (2) duration of flow exposure (4 versus 24 hours), (3) magnitude and characteristic of shear stress profiles, and (4) flow models (cone-and-plate versus pulsatile parallel plate), our finding in CuZn-SOD expression in response to PSS is in agreement with that Inou *et al.*. Moreover, we demonstrated that shear stress regulated Mn-DOS and CuZn-SOD expression in both BAEC and HAEC. Whether there exists a shear stress-responsive element in Mn-SOD gene remains undefined; however, a redox-sensitive mechanism was implicated in Mn-SOD promoter activity via a negative PI3K-akt-forkhead pathway and a positive PKC-NF-κB pathway [38].

Several studies have examined effects of SOD isoforms on endothelial function and atherogenesis. EC-SOD plays a significant protective role on arterial pressure, vascular function, or vascular levels of oxidative stress in spontaneous hypertensive rats 39. Similarly, cytosolic CuZn-SOD is atheroprotective, playing a critical role in limiting angiotensin II-induced endothelial cell dysfunction 40. The CuZn-SOD-deficient (CuZn-SOD(−/−)) mice showed an increased superoxide level and altered vascular responsiveness compared with the wild-type littermates [41]. The protein encoded Mn-SOD transmigrate to mitochondria. Mn-SOD-deficient mice (Mn-SOD(+/−) were reported to develop more atherosclerosis 37. However, the relative contribution of CuZn-SOD and Mn-SOD to dismutase superoxide anion in response to shear stress requires further investigations.

Previously, we reported that pulsatile flow significantly reduced the ratios of oxidatively modified forms of LDL relative to static conditions, whereas oscillating flow increased LDL oxidation [17], leading to up-regulation of adhesion molecules and recruitment of monocytes [42,43]. In this study, OSS increased the level of tyrosine nitration and oxidation products in LDL, whereas PSS decreased the levels of both tyrosine nitration and oxidation. Nitration of tyrosine residues by $ONOO^-$ resulted in a more hydrophilic residue, thus altering the structure of α helices of ApoB-100 of the LDL particles [44,45].

We analyzed LDL protein nitration at both protein and amino acid levels. The former was established by dot blots. Using anti-nitrityrosine antibody, we suspended LDL in mediums to assess LDL protein nitration. The latter was performed by liquid chromatography, electro ionization spray, and tandem mass spectrometry (LC/ESI/MS/MS). The proteomic approach allowed for identifying the specific apo B-100 tyrosine residue nitration in α and β helices as follows: α-1 (Tyr^{144}), α-2 (Tyr^{2524}), β-2 (Tyr^{3295}), α-3 (Tyr^{4116}), and β-2 (Tyr^{4211}) (*Hsiai, FRBM, 2007*). Both lipid peroxidation and protein nitration account for apoB-100 protein unfolding and consequential increase in modified LDL binding and uptake by endothelial cells.

Antioxidant gene expression is present in mouse aortic arch where disturbed flow, including oscillatory shear stress, develops. Perserini, Davies et al. reported a host of antioxidant gene expression from adult porcine aortic arch by genomics [46]. The authors suggested that there is an evolutionary benefit to favor a moderate level of atheroprotective gene expression in the athero-prone regions such as curvatures and bifurcations. In this context, our *in vitro* findings between oscillatory and pulsatile shear stress complement those of mouse genomic analysis.

In summary, our bifurcation model predicts the characteristics of shear stress in the PSS- and OSS-exposed regions of the arterial bifurcation. Explants of human coronary arteries

enabled us to assess the pathophysiological significance of this model in terms of Mn-SOD immunohisto-localization. Our findings strongly support the notion that pulsatile and oscillatory shear stress modulated spatial variations in Mn-SOD expression and that Mn-SOD plays an important role in LDL protein nitration.

Acknowledgments

The authors are grateful for Dr. Shan-Rong Shi and Lillian L. Young for their technical assistance with the coronary artery specimens in the Department of Pathology at the University of Southern California. The authors are also grateful for the native LDL provided by Dr. Mohamad Navab from the Division of Cardiology at UCLA David Gaffen School of Medicine. Finally, the authors would like to express appreciation for Stanley L. Hazen from the Cleveland Clinic for biochemical analyses. These studies were supported by AHA GIA 0655051Y (TKH), NIH HL068689 (TKH), NIH HL083015 (TKH), AHA Pre-Doctoral Fellowship 0615063Y (MR).

References

1. Ku DN, Giddens DP, Zarins CK, Glagov S. Pulsatile Flow and Atherosclerosis in the Human Carotid Bifurcation - Positive Correlation between Plaque Location and Low and Oscillating Shear-Stress. Arteriosclerosis 1985;5:293–302. [PubMed: 3994585]
2. Malek AM, Alper SL, Izumo S. Hemodynamic Shear Stress and Its Role in Atherosclerosis. Journal of American Medical Association 1999;282:2035–2042.
3. Davies PF, Dewey CF Jr, Bussolari SR, Gordon EJ, Gimbrone MA Jr. Influence of hemodynamic forces on vascular endothelial function. In vitro studies of shear stress and pinocytosis in bovine aortic cells. J Clin Invest 1984;73:1121–1129. [PubMed: 6707208]
4. Ku DN. Blood Flow in Arteries. Annu. Rev. Fluid Mech 1997;29:399–434.
5. De Keulenaer GW, Chappell DC, Ishizaka N, Nerem RM, Alexander RW, Griendling KK. Oscillatory and steady laminar shear stress differentially affect human endothelial redox state: role of a superoxide-producing NADH oxidase. Circ Res 1998;82:1094–1101. [PubMed: 9622162]
6. Landmesser U, Harrison DG. Oxidant stress as a marker for cardiovascular events - Ox marks the spot. Circulation 2001;104:2638–2640. [PubMed: 11723010]
7. Sorescu D, Weiss D, Lassegue B, Clempus RE, Szocs K, Sorescu GP, Valppu L, Quinn MT, Lambeth JD, Vega JD, Taylor WR, Griendling KK. Superoxide production and expression of nox family proteins in human atherosclerosis. Circulation 2002;105:1429–1435. [PubMed: 11914250]
8. Witztum JR. The oxidation hypothesis of atherosclerosis. Lancet 1994;344:793–795. [PubMed: 7916078]
9. Ziegler T, Bouzourene K, Harrison VJ, Brunner HR, Hayoz D. Influence of oscillatory and unidirectional flow environments on the expression of endothelin and nitric oxide synthase in cultured endothelial cells. Arterioscler Thromb Vasc Biol 1998;18:686–692. [PubMed: 9598825]
10. Esposito LA, Melov S, Panov A, Cottrell BA, Wallace DC. Mitochondrial disease in mouse results in increased oxidative stress. Proceedings of the National Academy of Sciences of the United States of America 1999;96:4820–4825. [PubMed: 10220377]
11. Wallace DC. Mitochondrial Genetics - a Paradigm for Aging and Degenerative Diseases. Science 1992;256:628–632. [PubMed: 1533953]
12. Li YB, Huang TT, Carlson EJ, Melov S, Ursell PC, Olson TL, Noble LJ, Yoshimura MP, Berger C, Chan PH, Wallace DC, Epstein CJ. Dilated Cardiomyopathy and Neonatal Lethality in Mutant Mice Lacking Manganese Superoxide-Dismutase. Nature Genetics 1995;11:376–381. [PubMed: 7493016]
13. Inoue N, Ramasamy S, Fukai T, Nerem RM, Harrison DG. Shear stress modulates expression of Cu/Zn superoxide dismutase in human aortic endothelial gels. Circulation Research 1996;79:32–37. [PubMed: 8925565]
14. Rush JWE, Laughlin MH, Woodman CR, Price EM. SOD-1 expression in pig coronary arterioles is increased by exercise training. American Journal of Physiology-Heart and Circulatory Physiology 2000;279:H2068–H2076. [PubMed: 11045939]

15. Tao J, Yang Z, Wang JM, Wang LC, Luo CF, Tang AL, Dong YG, Ma H. Shear stress increases Cu/Zn SOD activity and mRNA expression in human endothelial progenitor cells. Journal of Human Hypertension 2007;21:353–358. [PubMed: 17287843]

16. Woodman CR, Muller JM, Rush JWE, Laughlin MH, Price EM. Flow regulation of ecNOS and Cu/Zn SOD mRNA expression in porcine coronary arterioles. Am J Physiol: Heart Circ Physiol 1999;276:H1058–H1063.

17. Hwang J, Ing MH, Salazar A, Lassegue B, Griendling K, Navab M, Sevanian A, Hsiai TK. Pulsatile versus oscillatory shear stress regulates NADPH oxidase subunit expression - Implication for native LDL oxidation. Circ Res 2003;93:1225–1232. [PubMed: 14593003]

18. Li Y, Zheng J, Bird IM, Magness RR. Effects of pulsatile shear stress on signaling mechanisms controlling nitric oxide production, endothelial nitric oxide synthase phosphorylation, and expression in ovine fetoplacental artery endothelial cells. Endothelium-Journal of Endothelial Cell Research 2005;12:21–39. [PubMed: 16036314]

19. Fleming I, Fisslthaler B, Dixit M, Busse R. Role of PECAM-1 in the shear-stress-induced activation of Akt and the endothelial nitric oxide synthase (eNOS) in endothelial cells. Journal of Cell Science 2005;118:4103–4111. [PubMed: 16118242]

20. Chen YM, Medhora M, Falck JR, Pritchard KA, Jacobs ER. Mechanisms of activation of eNOS by 20-HETE and VEGF in bovine pulmonary artery endothelial cells. Am Jf Physiol Lung Cell Molec Physiol 2006;291:L378–L385.

21. Sowers JR, Epstein M, Frohlich ED. Diabetes, hypertension, and cardiovascular disease: an update. Hypertension 2001;37:1053–1059. [PubMed: 11304502]

22. Irani K. Oxidant signaling in vascular cell growth, death, and survival : a review of the roles of reactive oxygen species in smooth muscle and endothelial cell mitogenic and apoptotic signaling. Circ Res 2000;87(3)

23. Ramamurthi BBV. Arteriovenous malformations with a purely external carotid contribution. J Neurosurg 1966;25:643–647. [PubMed: 5925726]

24. Bharadvaj BKMR, Giddens DP. Steady flow in a model of the human carotid bifurcation. Part I--flow visualization. J Biomech 1982;15:349–362. [PubMed: 7118950]

25. Rouhanizadeh M, Lin TC, Arcas D, Hwang J, Hsiai TH. Spatial variations in shear stress in a 3-D bifurcation model at low Reynolds numbers. Annals of Biomedical Engineering 2005;33:1360–1374. [PubMed: 16240085]

26. Ku DN. Blood flow in arteries. Annual Rev Fluid Mechanics 1997;29:399–434.

27. Hsiai TK, Cho SK, Wong PK, Ing MH, Salazar A, Hama S, Navab M, Demer LL, Chih-Ming H. Micro sensors: Linking real-time oscillatory shear stress with vascular inflammatory responses. Annals of Biomedical Engineering 2004;32:189–201. [PubMed: 15008367]

28. Hsiai T, Cho SK, S H, Navab M, Demer LL, Ho CM. Endothelial Cell Dynamics under Pulsating Flow: Significance of High- vs. Low Shear Stress Slew Rates. Annals of Biomedical Engineeing 2002;30:646–656.

29. Nerem RM, Alexander RW, Chappell DC, Medford RM, Varner SE, Taylor WR. The study of the influence of flow on vascular endothelial biology. Am J Med Sci 1998;316:169–175. [PubMed: 9749558]

30. Papadaki, M.; McItire, LV. Methods in Molecular Medicine: Tissue Engineering Methods and Protocols. In: MJ, R.; Yarmush, ML., editors. Quantitative Measurement of Shear-Stress Effects on Endothelial Cells. Totowa, NJ: Humana Press Inc.; 1998. p. 577-593.

31. Hodis HN, Kramsch DM, Avogaro P, Bittolobon G, Cazzolato G, Hwang J, Peterson H, Sevanian A. Biochemical and Cytotoxic Characteristics of an in-Vivo Circulating Oxidized Low-Density-Lipoprotein (Ldl-). J Lipid Res 1994;35:669–677. [PubMed: 8006522]

32. Brennan ML, Wu W, Fu X, Shen Z, Song W, Frost H, Vadseth C, Narine L, Lenkiewicz E, Borchers MT, Lusis AJ, Lee JJ, Lee NA, Abu-Soud HM, Ischiropoulos H, SL H. A tale of two controversies: defining both the role of peroxidases in nitrotyrosine formation in vivo using eosinophil peroxidase and myeloperoxidase-deficient mice, and the nature of peroxidase-generated reactive nitrogen species. J Biol Chem 2002;277:17415–17427. [PubMed: 11877405]

33. Hsiai TK, Hwang J, Barr ML, Correa A, Hamilton R, Alavi M, Rouhanizadeh M, Cadenas E, Hazen SL. Hemodynamics influences vascular peroxynitrite formation: Implication for low-

density lipoprotein apo-B-100 nitration. Free Radical Biology and Medicine 2007;42:519–529. [PubMed: 17275684]

34. Madamanchi NR, Vendrov A, Runge MS. Oxidative stress and vascular disease. Arterioscler Thromb Vasc Biol 2005;25:29–38. [PubMed: 15539615]
35. Boveris A, Cadenas E, Stoppani AO. Role of ubiquinone in the mitochondrial generation of hydrogen peroxide. Biochem J 1976;156:435–444. [PubMed: 182149]
36. Bernal-Mizrachi C, Gates AC, Weng S, Imamura T, Knutsen RH, DeSantis P, Coleman T, Townsend RR, Muglia LJ, Semenkovich CF. Vascular respiratory uncoupling increases blood pressure and atherosclerosis. Nature 2005;435:502–506. [PubMed: 15917810]
37. Ohashi M, Runge MS, Faraci FM, Heistad DD. MnSOD deficiency increases endothelial dysfunction in ApoE-deficient mice. Arterioscler Thromb Vasc Biol 2006;26:2331–2336. [PubMed: 16873728]
38. Abid MR, Schoots IG, Spokes KC, Wu SQ, Mawhinney C, Aird WC. Vascular endothelial growth factor-mediated induction of manganese superoxide dismutase occurs through redox-dependent regulation of forkhead and I kappa B/NF-kappa B. Journal of Biological Chemistry 2004;279:44030–44038. [PubMed: 15308628]
39. Chu Y, Alwahdani A, Iida S, Lund DD, Faraci FM, Heistad DD. Vascular effects of the human extracellular superoxide dismutase R213G variant. Circulation 2005;112:1047–1053. [PubMed: 16087794]
40. Didion SP, Kinzenbaw DA, Faraci FM. Critical role for CuZn-superoxide dismutase in preventing angiotensin II-induced endothelial dysfunction. Hypertension 2005;46:1147–1153. [PubMed: 16216984]
41. Didion SP, Ryan MJ, Didion LA, Fegan PE, Sigmund CD, Faraci FM. Increased superoxide and vascular dysfunction in CuZnSOD-deficient mice. Circ Res 2002;91:938–944. [PubMed: 12433839]
42. Hsiai TK, Sung CK, Susan HY, Jin LS, Honda H, Reddy ST, Navab M, Fogelman AM, Demer LL, Ho CM. Pulsatile vs. oscillatory flow profiles have opposite effects on monocyte adhesion to OX-PAPC treated endothelial cells. Circulation 2000;102 185-185.
43. Hsiai TK, Cho SK, Wong PK, Ing M, Salazar A, Sevanian A, Navab M, Demer LL, Ho CM. Monocyte recruitment to endothelial cells in response to oscillatory shear stress. Faseb Journal 2003;17:1648–1657. [PubMed: 12958171]
44. Asatryan L, Hamilton RT, Isas JM, Hwang J, Kayed R, Sevanian A. LDL phospholipid hydrolysis produces modified electronegative particles with an unfolded apoB-100 protein. Journal of Lipid Research 2005;46:115–122. [PubMed: 15489541]
45. Hwang J, Rouhanizadeh M, Hamilton RT, Lin TC, Eiserich JP, Hodis HN, Hsiai TK. 17 beta-Estradiol reverses shear-stress-mediated low density lipoprotein modifications. Free Radical Biology and Medicine 2006;41:568–578. [PubMed: 16863990]
46. Passerini AG, Polacek DC, Shi CZ, Francesco NM, Manduchi E, Grant GR, Pritchard WF, Powell S, Chang GY, Stoeckert CJ, Davies PF. Coexisting proinflammatory and antioxidative endothelial transcription profiles in a disturbed flow region of the adult porcine aorta. Proceedings of the National Academy of Sciences of the United States of America 2004;101:2482–2487. [PubMed: 14983035]

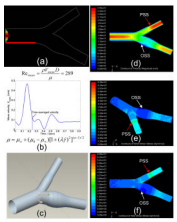

Fig. 1.

Spatial variations in shear stress. **(a)** The boundary condition. **(b)** Carreau model for non-Newtonian blow flow (*Bird R. B., Armstrong R. C., Hassager O., 1977. Dynamics of Polymeric Liquids, Vol. 1, Fluid Mechanics New York: Wiley.470 PP.*), where μ represents viscosity, γ represents the shear rate, μ_0 represents the zero shear rate limit viscosity, μ_∞ represents the infinite shear rate limit viscosity, λ represents the relaxation time constant, and n is the power law index. **(c)** Reconstruction of carotid artery. **(d)** An instantaneous velocity profile (t = 0.244 s). **(e)** Anterior-oblique angle of shear stress profile at an instantaneous moment with the mean Reynolds number of 289. **(f)** Top view of shear stress profile. White arrow indicates the point of flow separation.

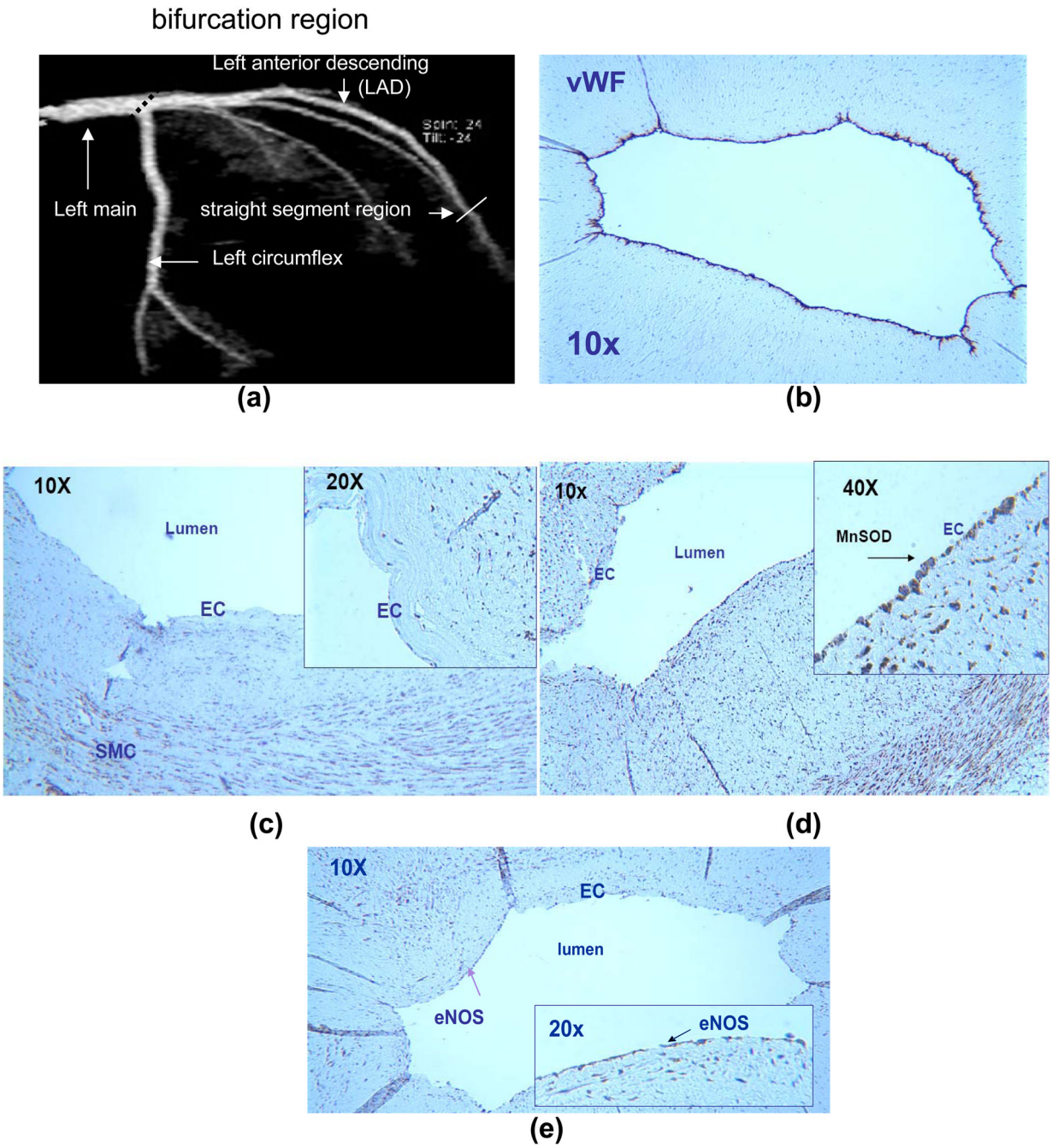

Fig. 2.

Mn-SOD immunostaining of a section of left coronary artery. **(a)** A representative left coronary artery and its branches. **(b)** von Willebrand Factor (vWF) staining for EC. **(c)** At the left main bifurcation (OSS-exposed region), Mn-SOD staining was absent in the luminal EC. **(d)** In straight segment of LAD (PSS-exposed region), Mn-SOD staining was prevalent throughout the entire luminal EC. **(e)** eNOS staining was positive. This section was previously reported *(Hsiai et al. (provide ref))*.

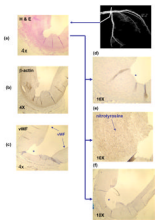

Fig. 3.

Nitrotyrosine immunostaining of left main coronary arterial bifurcation. **(a)** Counterstaining with Hemotoxylin. **(b)** β-actin forsmooth muscle cells (SMC). **(c)** von Willebrand factor(vWF) for EC. Note that "*" indicates the lumen that was denuded in EC. **(d)** MnSOD staining was absent in the luminal endothelium. **(e)** Nitrotyrosine staining was prevalent in the SMC. **(f)** eNOS staining was absent.

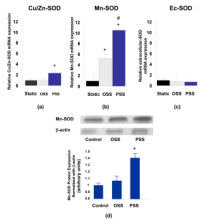

Fig. 4.

SOD isofrom expression in BAEC in response to oscillatory (OSS) and pulsatile shear stress. Cu/Zn-, Mn-, and extracellular-SOD mRNA expression was normalized to 18s RNA (**P* < 0.05 in comparison to the static samples, n=3). **(a)** Cu/Zn-SOD expression was up-regulated by 2.3-fold in response to PSS. **(b)** Mn-SOD mRNA expression was up-regulated by 5-fold in response to OSS and by 11.4-fold to PSS. **(c)** EC-SOD remained relatively unresponsive to shear stress, (**P* < 0.05 versus static, #*P* < 0.05 versus OSS, n=3). **(d)** Mn-SOD protein expression. The increased in Mn-SOD expression was not statistically significant in response to OSS. PSS up-regulated Mn-SOD expression by 1.4-fold (* P < 0.05, n = 4).

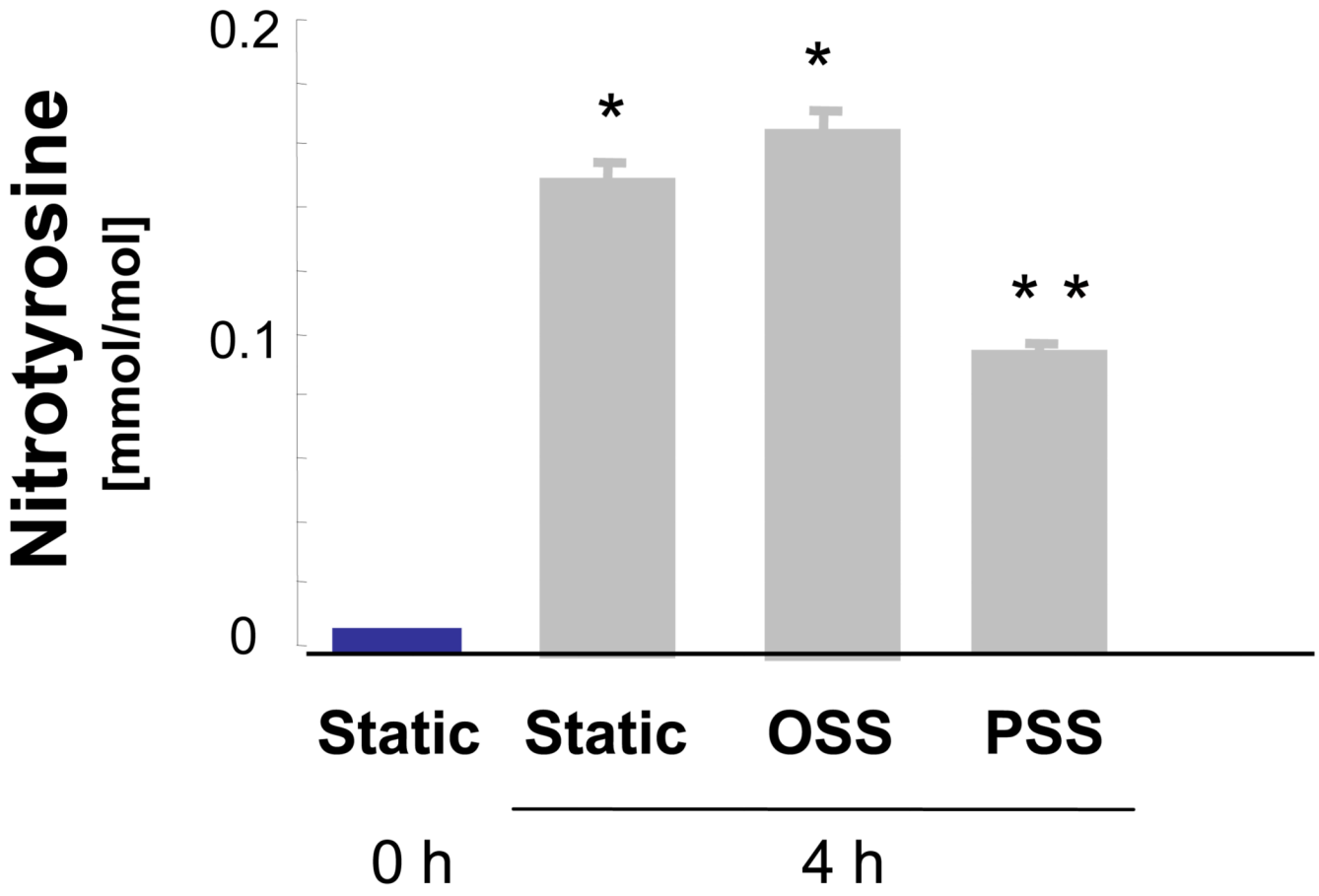

Fig. 5.

Liquid chromatography/electron spray ionization/mass spectroscopy/mass spectroscopy (LC/ESI/MS/MS) analyses of LDL protein nitration as a finger print of nitrotyrosine formation. LDL nitration occurred when BAEC were treated with native LDL at 4 h. OSS further increased the level of LDL nitration whereas PSS decreased the level at 4 h (*P < 0.05 versus static at 0h, **P < 0.05 versus OSS, n=4).

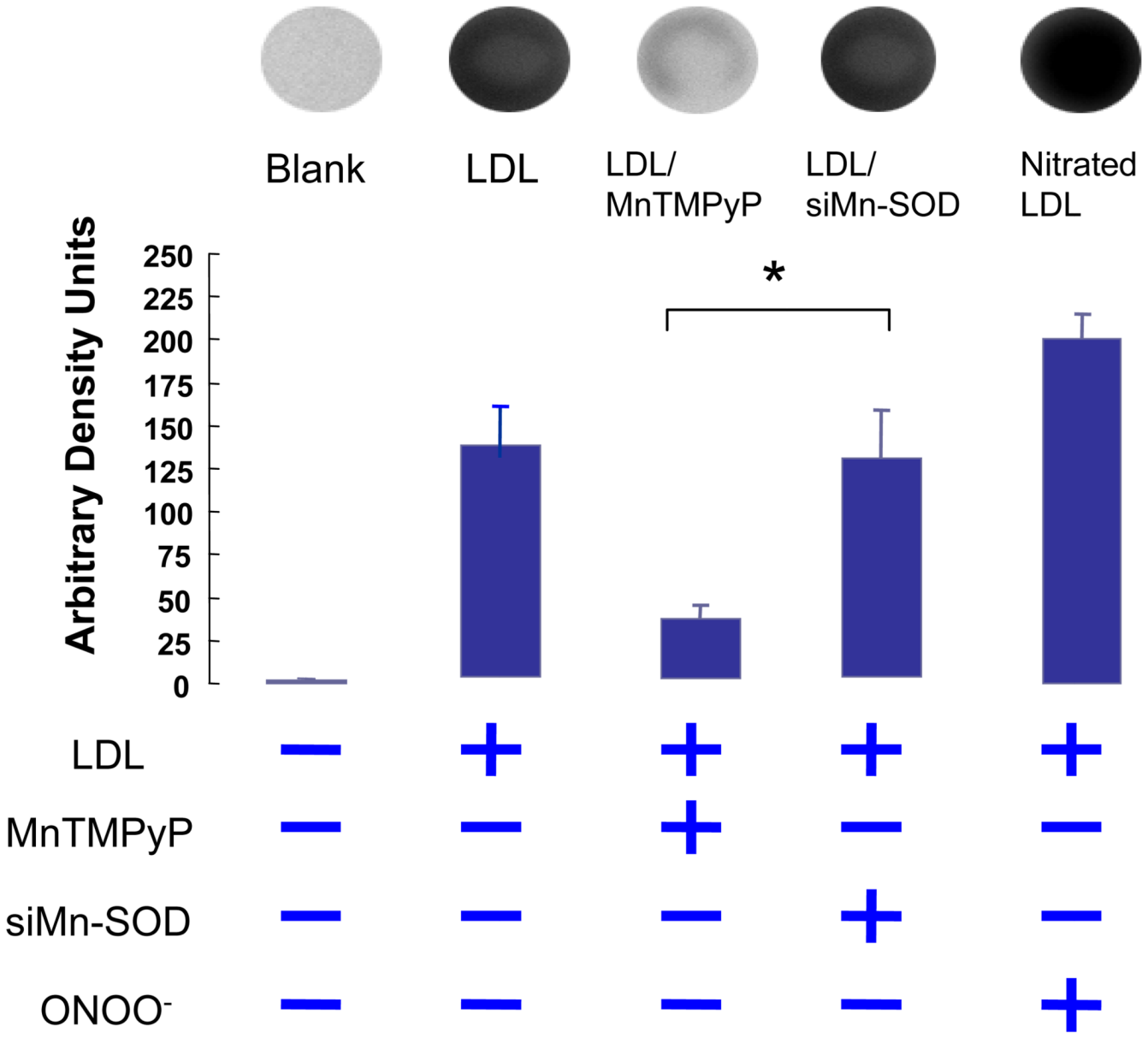

Fig. 6.

Dot Blot analyses of extracellular nitrotyrosine levels in the presence of native LDL. Blank refers to samples without LDL treatment. Native LDL induced an increase in LDL nitrotyrosine level. Addition of Mn-SOD mimetic (MnTMPyP) significantly attenuated the nitrotyrosine level. Positive control indicates samples treated with ONOO-. The nitrotyrsoine level in siMn-SOD treated HAEC was significantly higher than that of MnTMPyP-treated HAEC. The differences between siMn-SOD plus LDL-treated samples and the LDL-treated were statistically insignificant (P >0.05, n=4).

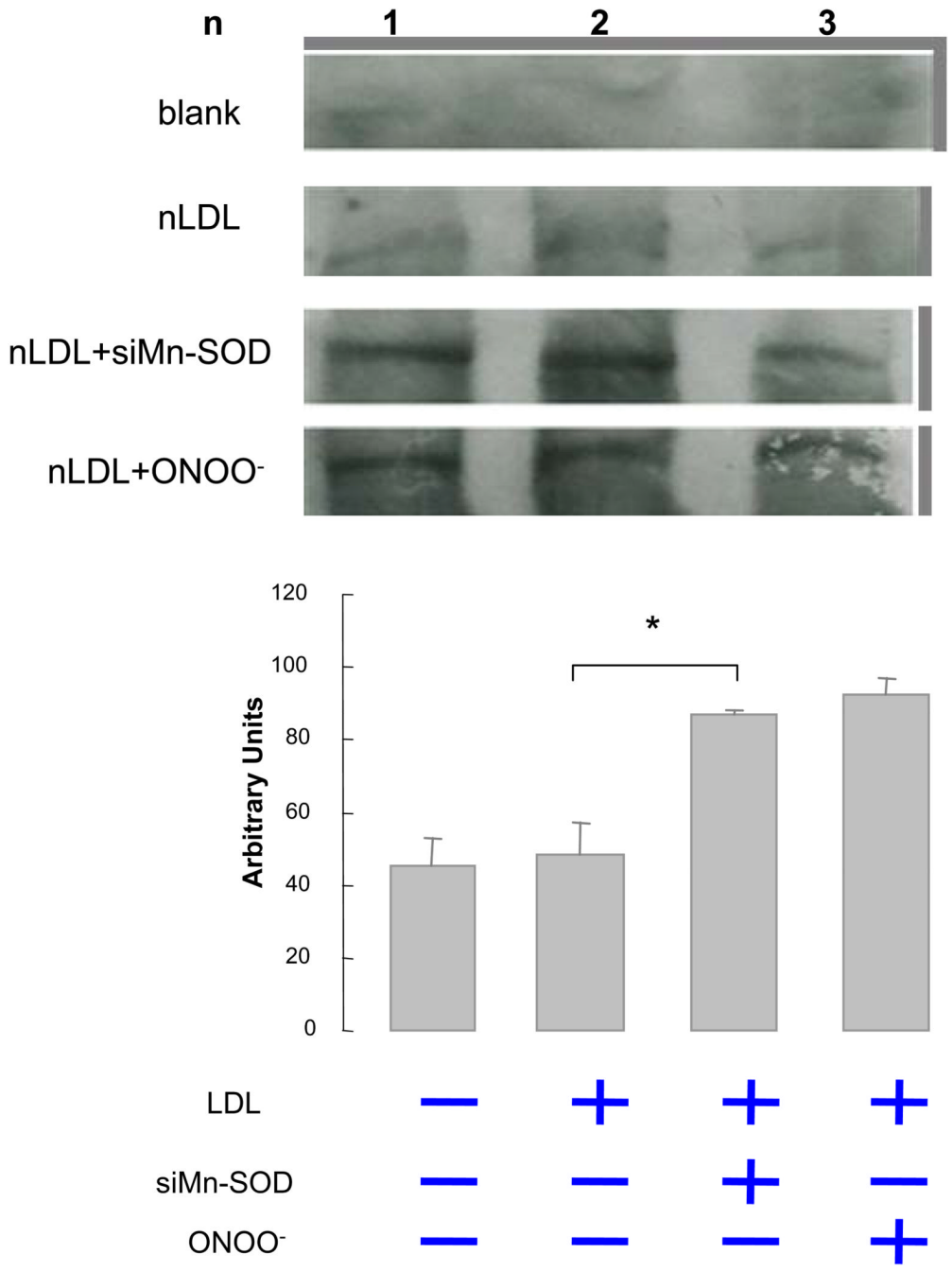

Fig. 7.

Western analysis of intracellular nitrotyrosine levels in native LDL-treated BAEC. Silencing Mn-SOD significantly increased nitrotyrosine level. Blank refers to samples without LDL treatment. Positive control indicates samples treated with ONOO- ($P < 0.05$, n=3).